Published in final edited form as:
Neurobiol Dis. 2008 February ; 29(2): 232–241.

The high affinity peripheral benzodiazepine receptor ligand DAA1106 binds to activated and infected brain macrophages in areas of synaptic degeneration:

implications for PET imaging of neuroinflammation in lentiviral encephalitis

Sriram Venneti, **Guoji Wang**, and **Clayton A. Wiley**
From the Department of Pathology, University of Pittsburgh School of Medicine, Pittsburgh, Pennsylvania, USA

Abstract

HIV encephalitis (HIVE) is characterized by neurodegeneration mediated by toxins derived from infected and activated brain macrophages. Since the peripheral benzodiazepine receptor (PBR) is abundant on brain macrophages, we hypothesized that [^{3}H]DAA1106, a new PBR ligand, can label infected and activated brain macrophages in HIVE. Using cell culture and postmortem brain tissues from HIVE and a macaque model of HIVE, we show that [^{3}H]DAA1106 binds with high affinity to activated and infected macrophages in regions of synaptic damage. Further, binding affinity reflected by lower K_D (dissociation constant) values and the B_{max} (total number of binding sites) to K_D ratios reflective of ligand-binding potential, were significantly higher with [^{3}H]DAA1106 compared to the extensively characterized PBR ligand [^{3}H](R)-PK11195. These data suggest that DAA1106 binds with high affinity to activated and infected brain macrophages and possesses binding characteristics beneficial for *in vivo* use in the detection and clinical monitoring of HIVE using positron emission tomography.

Keywords

Peripheral benzodiazepine receptor; Macrophages; PET; DAA1106; HIV encephalitis; PK11195; SIV encephalitis

Introduction

HIV-associated neurological abnormalities are seen in approximately 25% of terminally ill AIDS patients (Cinque et al., 1997, Dore et al., 1999). Deficits observed in these individuals range from minor cognitive impairment, motor and psychiatric dysfunctions to frank dementia thought to result from neuronal damage (Nath et al., 2006). Neuronal and synaptic injury is attributed to viral proteins and toxic products derived from HIV-infected and activated infiltrating macrophages (Ellis et al., 2007). These infected and activated macrophages manifest in the brain as microglial nodules, multinucleated giant cells and perivascular macrophage infiltrates, histopathologically referred to as HIVE. SIV infection in macaques has been used to model HIVE with a variable percentage of macaques developing SIVE

Corresponding author: Dr. Clayton A. Wiley, Presbyterian University Hospital, Neuropathology Division, 200 Lothrop Street A515, Pittsburgh, PA, USA 15213. Phone: (412) 647-0765. FAX: (412) 647-5602. Email address: wiley1@pitt.edu.

(Lackner et al., 1991). Since activated and infected macrophages in the brain are central to the pathology of lentiviral encephalitis, our goal is to image these cells *in vivo* using PET to enable the detection and progression of lentiviral encephalitis in the macaque model and eventually in human subjects.

Brain macrophages can be imaged *in vivo* using PET by taking advantage of increased expression of the peripheral benzodiazepine receptor (PBR) (Banati, 2002). Unlike the central benzodiazepine receptor, PBR is expressed at relatively low levels in the normal brain on resting brain macrophages and astrocytes (Cagnin et al., 2002). PK11195, the prototype PBR ligand, has been shown to cross the blood brain barrier and achieve specific binding to brain macrophages in both animal models and human subjects with neuroinflammation (Banati, 2002).

We and others have shown that activated brain macrophages can be labeled with [^{3}H](R)-PK11195 in SIVE (Mankowski et al., 2003, Venneti et al., 2004) and that [^{11}C](R)-PK11195 can be used to image activated brain macrophages *in vivo* using PET in macaques that develop encephalitis (Venneti et al., 2004). However, translation of these studies to human subjects has been less promising. [^{11}C](R)-PK11195 PET retention in the brain did not differ between HIV infected patients on retroviral drugs with and without neurological deficits (Hammoud et al., 2005, Wiley et al., 2006). These findings may be in part due to decreased brain inflammation seen in neurologically impaired HIV infected subjects on antiretroviral therapy (ART) without frank dementia (Gray et al., 2003b, Gray et al., 2003a). It is also possible that [^{11}C](R)-PK11195 shows low sensitivity of in detecting milder forms of neuroinflammation. Ligands that bind to PBR with higher affinity compared to PK11195 may show greater sensitivity in detecting milder forms of neuroinflammation. DAA1106 [N-(2,5-dimethoxybenzyl)-N-(4-uoro-2-phenoxyphenyl)-acetamide] is an aryloxyanilide derivative, that binds with higher affinity to PBR compared to PK11195 (Chaki et al., 1999, Zhang et al., 2003, Maeda et al., 2004). We hypothesized that DAA1106 would label activated brain macrophages in encephalitic brain tissues with higher binding affinity when compared to that of PK11195. We show that [^{3}H]DAA1106 binding is higher in lentiviral encephalitis with greater B_{max}/K_D ratios compared to [^{3}H](R)-PK11195 correlating with infected and activated macrophages in areas with synaptic damage. These data suggest that DAA1106 possesses binding characteristics that could lead to improved PET imaging of lentiviral encephalitis.

Methods

Archival human and macaque brain tissue

Brain tissue was obtained from the University of Pittsburgh brain bank. Neuropathological microscopic analysis was performed in all human and macaque brain tissues. Only brains that showed no evidence of opportunistic infections were chosen for analysis. Encephalitis was diagnosed on the basis of distribution of macrophage infiltrates, microglial nodules, multinucleated giant cells and abundant macrophages that immunostained for HIV gp41 or SIV gp110 in human and macaque cases respectively (Budka, 1991, Lackner et al., 1991). Frozen tissue from the basal ganglia of patients with HIVE (n=5), HIV infected, non-encephalitis (n=5) and non-infected controls (n=3) and from the frontal cortex of macaques with SIVE (n=3), SIV infected, non-encephalitis (n=4) and non-infected controls (n=3) were used (Table 1).

Tissue culture experiments

Primary human macrophage cultures were isolated from peripheral blood mononuclear cells isolated from HIV and Hepatitis B seronegative buffy coats obtained from the blood bank (Central Blood Bank, Pittsburgh, PA) using established protocols (Bergamini et al., 1999) and

cultured for 7 days. Human fetal brain tissue was gathered according to the standards of the University of Pittsburgh ethics and biosafety guidelines. Primary human astrocyte and microglial cell were isolated as per established protocols (Lee et al., 1992, Barami et al., 2001). Astrocytes and microglia were treated with 1μg/ml LPS (Sigma, Sr. Louis, MO) for 48hrs. Astrocytes were additionally activated with 100 μM dibutyryl cyclic AMP (dB-CAMP) (Sigma) for 48hrs in parallel cultures. dB-CAMP has been extensively used to model in cell culture the morphological and proliferative changes seen in reactive astrocytosis(Padmanabhan et al., 1999, Abe et al., 2000). Mitochondrial extracts were obtained from primary human macrophages, microglia and astrocytic cultures utilizing a kit obtained from Pierce (Rockford, IL) based on the metrizamide gradient centrifugation method that yields 97.71% pure mitochondrial preparations (Taylor et al., 2003).

Filtration radioligand binding assays

(a) Saturation binding curves—Homogenized brain tissue samples (total protein concentration ranging from 150 to 200 μg) were incubated with 0.2 to 25 nM [^{3}H]-DAA1106 (sp. act., 80 Ci/mmol; American Radiolabeled Chemical, St Louis, MO) or 0.5-100 nM [^{3}H](R)-PK11195 (sp. act., 89.9 Ci/mmol; NEN Life Sciences Products, Boston, MA) at 4°C for 2 hr in a final volume of 250 μl of HEPES (4°C, pH 7.4). This was defined as total binding. Nonspecific binding was excluded by the inclusion of 10 μM DAA11106 or 10 μM PK11195 respectively.

(b) Specific binding analyses in mitochondrial extracts—Mitochondrial extracts derived from primary human astrocytes, macrophages and microglia were incubated with 1 nM [^{3}H]DAA1106 and non-specific binding was excluded by the inclusion of 1 μM DAA1106.

In both the above experimental conditions the reaction was terminated by filtration through glass fiber filters (Brandel, Gaithersburg, MD) by the addition of HEPES (4°C, pH 7.4) in a vacuum cell harvester (Brandel). Filter bound radioactivity was counted in a liquid scintillation spectrometer (Perkin Elmer Life Sciences, Wellesley, MA). Specific binding at each concentration of ^{3}H-ligand was defined as the difference between total binding and nonspecific binding. Specific binding in brain tissues ranged from 80-90% of total binding (nonspecific binding values at 1nM [^{3}H]-ligand were ~ 8% in macaque and ~ 10% of total binding in human brain tissues respectively). All samples were run in duplicate. B_{max} (fmols/mg protein) and K_D (nM) were determined using PRISM software (Graphpad, San Diego, CA). B_{max}/K_D ratios (representing a measure of the binding potential of each ligand) were obtained to compare both ligands.

Immunohistochemistry

Immunostaining and laser confocal microscopic imaging was performed as described previously (Venneti et al., 2004). Paraffin sections containing the frontal cortex in the same macaques from which frozen tissue was obtained were used. Sections were stained with mouse monoclonal antibodies against CD68 (marker for activated macrophages, 1:50,000, DAKO, Carpinteria, CA) or MAP-2 (1:1500, Sternberger Inc., Lutherville, MD), or synaptophysin (1:100, DAKO), or GFAP (1:500, DAKO) or rabbit polyclonal antibody against the SIV envelope gp110 (5 μg/ml, gift from Dr. Kelly Stefano Cole, University of Pittsburgh, Pittsburgh, PA) with secondary Cy5-conjugated goat anti-mouse IgG and Cy3-conjugated goat anti-rabbit IgG (1:200, Jackson ImmunoResearch Laboratories, Inc.). Immunostained sections were scanned and quantified on a laser confocal microscope equipped with an argon laser with 458, 477, 488, and 514 nm primary emission lines (LSM 150; Carl Zeiss GmbH, Heidelberg, Germany). Each section was scanned along the *z*-axis to define the middle optical plane used in quantification (262,144 pixels/plane; 1 pixel = 0.25 mm^2). Scanning parameters such as laser power aperture, gain, and photomultiplier tube settings were kept constant for each

wavelength. An individual blinded to the experimental design imaged ten areas (x40) encompassing 106,100 μm^2. For each cell phenotype scanned, contribution to signal intensity from autofluorescence was minimized using a threshold that was kept constant. In each area the average pixel fluorescence along with the pixel counts for a given cell phenotype marker that exceeded the threshold were enumerated. The average pixel fluorescence was multiplied by the total number of pixels to measure the total fluorescence for that cell phenotype marker in that area. The total fluorescence values determined from the ten scanned areas in one brain region were averaged to represent a measure of the cell phenotype in that brain region.

Autoradiography

Autoradiography was performed as described(Venneti et al., 2004). Briefly, 15 μm thick frozen brain sections were placed on Superfrost^{Tm} glass slides (Sigma) and incubated in 50 mM HEPES containing 1 nM [^{3}H]DAA1106 for 30 min. Specificity of binding was ensured by the inclusion of 1 μM DAA1106 in parallel sections. The sections were mounted with a layer of autoradiographic LM-1 emulsion (Amersham, UK), were developed after 4 weeks. We combined immunostaining with autoradiography to evaluate the cellular localization of [^{3}H] DAA1106. Sections were first immunostained and then processed for autoradiography, following which they were imaged on the confocal microscope.

Statistical analysis

Data were analyzed using PRISM software (Graphpad, San Diego, CA). Students *t* test or one-way ANOVA tests with post-test Bonferroni correction with 95% confidence intervals were used to analyze data. Non parametric correlations using 95% confidence intervals were performed to quantify the relationship between [^{3}H]DAA1106 binding and various immunohistochemical markers represented by *r*, the Spearman's coefficient.

Results

[^{3}H]DAA1106 binding is higher in lentiviral encephalitis compared to controls

B_{max} and K_D values reflective of the total number of binding sites per mg protein and binding affinity of [^{3}H]DAA1106 to PBR respectively were determined in post mortem brain tissue derived from the basal ganglia from HIVE, HIV infected non-encephalitis and age-matched non-infected cases. B_{max} with [^{3}H]DAA1106 was significantly higher in HIVE compared to controls (Figure 1A-C & table 3, p=0.0003). K_D, the affinity of binding of [^{3}H]DAA1106 did not differ in all these conditions (Figure 1D & table 3, p=0.0712). Similar results were obtained in SIVE compared to SIV infected non-encephalitis and control uninfected tissues obtained from the frontal cortex (Figure 2C & table 3, B_{max}, p=0.0038 and **2D,** K_D, p=0.2492). These results were confirmed by performing autoradiography on brain tissue obtained from the frontal cortex of SIVE macaques (Figure 2A and B).

[^{3}H]DAA1106 binding is higher in activated macrophages compared to controls in cell culture

We compared changes in [^{3}H]DAA1106 binding in primary human macrophages, microglia and astrocytes with and without activation. Primary human microglia and macrophages were activated with LPS (Figure 3B and C, untreated controls shown in insets). Astrocytic cultures were activated with dB-cAMP (Figure 3A, untreated control shown in inset). Astrocytes treated with LPS served as additional controls. As PBR is a mitochondrial receptor (Casellas et al., 2002), we assessed changes in [^{3}H]DAA1106 binding in mitochondrial extracts obtained from each of these conditions. [^{3}H]DAA1106 binding did not differ significantly in astrocytes activated with dB-cAMP or LPS from untreated cultures (Figure 3D). In contrast, [^{3}H] DAA1106 binding was significantly higher in both LPS-activated macrophage and microglial cultures compared to untreated controls and all the astrocytic conditions (Figure 3D).

[^{3}H]DAA1106 binding corresponds to activated and infected macrophages in SIVE

We wanted to determine the relative contributions of astrocytes and activated brain macrophages to [^{3}H]DAA1106 binding. Since macrophages are the predominant infected cells in the brain in lentiviral encephailitis (Ellis et al., 2007), we also determined the association between infected macrophages and [^{3}H]DAA1106 binding in the brain. We combined immunostaining for astrocytes (GFAP), activated brain macrophages (CD68) and the SIV envelope protein gp110 with [^{3}H]DAA1106 autoradiography on frozen brain sections obtained from the frontal cortex of SIVE macaques. [^{3}H]DAA1106 binding overlapped with CD68 labeled activated macrophages (Figure 4A) and SIV-infected macrophages (Figure 4C), but not with GFAP labeled astrocytes (Figure 4B). Similar results including colocalization of HIV infected cells with [^{3}H]DAA1106 autoradiography were seen in HIVE brain tissues (Figure 4D).

Next, we tested whether [^{3}H]DAA1106 binding in homogenized brain tissue correlated with the abundance of astrocytes or activated macrophages or SIV-infected macrophages labeled with GFAP, CD68 and SIV gp110 respectively. Each cell-type was quantified using confocal microscopy and correlated with [^{3}H]DAA1106 B_{max} values obtained from the same brain regions in the same macaques. [^{3}H]DAA1106 binding correlated significantly with the abundance of SIV-infected macrophages (r=0.9646; p=0.0084) and activated macrophages (r=0.8308; p=0.0160) but weakly with the abundance of GFAP-stained astrocytes (r=0.6755; p=0.0958) (Table 2).

Decreases in the presynaptic protein SYN and the postsynaptic protein MAP-2 correlate with increases in [^{3}H]DAA1106 binding

The presynaptic protein SYN and the postsynaptic protein MAP-2 were quantified in macaque brain tissues. Both proteins were decreased in SIVE compared to controls (Figure 5). Decreases in SYN (r= - 0.7806, p=0.0383) and MAP-2 (r= - 0.7868, p=0.0205) correlated with increases in [^{3}H]DAA1106 B_{max} values (Table 2)

Binding affinities (reflected by low K_D values) and B_{max}/K_D ratios with [^{3}H]DAA1106 are higher than that with [^{3}H](R)-PK1195 in lentiviral encephalitis

B_{max} and K_D values with [^{3}H]DAA1106 and [^{3}H](R)-PK1195 were compared in macaque and human tissues. B_{max} values did not differ between [^{3}H]DAA1106 and [^{3}H](R)-PK1195 in all conditions (table 3). K_D values with [^{3}H]DAA1106 were significantly lower compared to [^{3}H](R)-PK1195 in all conditions assessed, suggesting higher affinity with DAA1106 compared to PK11195 (table 3). B_{max}/K_D ratios representing the binding potential of either ligand, was significantly higher with both [^{3}H]DAA1106 and [^{3}H](R)-PK11195 in HIVE compared to HIV non-encephalitis and age-matched non-infected controls (Figure 6A). Within each group B_{max}/K_D ratio with [^{3}H]DAA1106 was significantly higher compared to [^{3}H](R)-PK11195 with the greatest differences obsereved in HIVE. Similar results were observed in SIVE compared to controls (Figure 6B).

Discussion

Despite the absence of productive infection of neurons lentiviral encephalitis is characterized by progressive neurodegeneration. Neuronal and synaptic damage has been hypothesized to be mediated by neurotoxins derived from activated and infected macrophages that infiltrate the brain (reviewed in (Ellis et al., 2007)). Since brain macrophages are key to the pathogenesis of lentiviral encephalitis, imaging these cells *in vivo* will enable detection and progression of encephalitis. DAA1106 is a ligand that binds to PBR enriched in activated macrophages, but present in low levels in the normal brain on astrocytes and resting brain macrophages ((Banati, 2002, Venneti et al., 2006)). Our data show that both HIVE and SIVE brain tissues have

significantly higher [^{3}H]DAA1106 binding compared to controls, which in macaque tissues correlated with the abundance of activated and SIV-infected macrophages, but not with the abundance of reactive astrocytes. Further, decreases in both the presynaptic protein SYN and the postsynaptic protein MAP-2 correlated with increases in [^{3}H]DAA1106 binding in SIVE, suggesting that regions showing increased [^{3}H]DAA1106 binding labeled areas with synaptic damage. Finally, the binding potential of [^{3}H]DAA1106, reflected by the B_{max}/K_D ratio was significantly higher when compared with that of [^{3}H](R)-PK11195 in the same brain region in the same cases in the both HIVE and SIVE suggesting that DAA1106 possesses better binding characteristics over PK11195 for labeling activated and infected macrophages in lentiviral encephalitis. The choice of brain tissues as the basal ganglia in human subjects and the frontal cortex was based on tissue availability. Histopathology in both human subjects and macaques suggest that lentiviral encephalitis does not target a specific area of the brain. However, prominent involvement of basal ganglia has been suggested in human subjects (Brew et al., 1995), while in macaques a more diffuse pattern of disease has been noted (Lackner et al., 1991). Despite these differences, the pathology of disease is both humans and macaques is similar, suggesting that our data obtained from the basal ganglia of human subjects and from the frontal cortex of macaques are comparable.

We have shown that [^{11}C](R)-PK11195 can image activated brain macrophages in macaques with terminal AIDS that develop SIVE using PET (Venneti et al., 2004). However, no differences were seen in [^{11}C](R)-PK11195 brain retention in HIV infected individuals with or without neurological deficits (Hammoud et al., 2005, Wiley et al., 2006). Although, subjects in these two studies showed neurological impairments, none of the patients had frank dementia. Therefore, none of these subjects would be expected to have HIVE. Further, most of the patients in both these studies were on ART. Indeed, the incidence of HIVD has been reported to decrease in HIV infected patients on ART. However, the prevalence of HIVD may increase due to the longer life spans of HIV infected patients on ART (Geraci et al., 2001, Valcour et al., 2004). The neuropathology seen in these patients is also different from frank encephalitis: subtle degeneration of dendritic arbors and interneuron populations (Langford et al., 2003), suggesting that activation of brain macrophages in these subjects may be less severe until progression to encephalitis and frank dementia. Analogous to these findings, [^{11}C](R)-PK11195 retention in the brain does not differ in normal subjects when compared with patients with minor cognitive impairment, a condition thought to progress to Alzheimer's disease in approximately 50% of subjects (Schuitemaker et al., 2004, Schuitemaker et al., 2006). These data suggest that [^{11}C](R)-PK11195 may not be able detect milder forms of neuroinflammation highlighting the significance of developing newer ligands that show high specificity and sensitivity for PET imaging of activated brain macrophages in HIVE. The B_{max}/K_D ratio (reflective of the binding potential of a PET ligand (Mintun et al., 1984)) with [^{3}H]DAA1106 was significantly higher when compared with that of [^{3}H](R)-PK11195 in both SIVE and HIVE, suggesting that DAA1106 may be able to address some of these issues. However, It is also possible that the lack of increase of [^{11}C](R)-PK11195 binding in HIV-infected patients with neurological signs could be due to the effects of ART in potentially decreasing brain inflammation, in which case either ligand would be insensitive. Future studies in SIV-infected macaques and HIV-infected patients will be able to address these issues.

The major cell type that DAA1106 binds to in neuroinflammatory conditions is not known. We show that [^{3}H]DAA1106 binds mainly to activated and infected brain macrophages in SIVE brain tissue. This is further substantiated by significant correlations of [^{3}H]DAA1106 binding with areas of synaptic damage, since activated and infected macrophages are thought to mediate synaptic injury in lentiviral encephalitis (Masliah et al., 1997, Ellis et al., 2007). Some studies report significant contributions from astrocytes to [^{3}H](R)-PK11195 binding in animal treated with neurotoxins and tissue culture systems (Itzhak et al., 1994, Kuhlmann et al., 2000, Chen et al., 2004). However, we found that the majority of [^{3}H]DAA1106 binding

correlated with activated and infected macrophages in SIVE brain tissues correlating weakly with the abundance of astrocytosis.

PBR is an outer mitochondrial membrane protein in a hetero-oligomeric complex comprised of the voltage-dependent anion channel and the adenine nucleotide carrier (Casellas et al., 2002). We found increases in [^{3}H]DAA1106 binding in mitochondrial fractions derived from LPS activated macrophages and microglia compared to controls and activated and control astrocytes. Further, no differences were observed in [^{3}H]DAA1106 binding between LPS activated primary macrophages and microglia suggesting that PBR binding sites do not differ between activated resident microglia and activated infiltrating macrophages in the brain.

PK11195 has been extensively used to image activated brain macrophages in several neurological disorders. However, the specific binding signal with [^{11}C](R)-PK11195 is generally low and challenging to quantitative with typical PET image noise levels (Petit-Taboue et al., 1991, Groom et al., 1995, Banati et al., 2000, Pappata et al., 2000). Another consideration is that [^{11}C](R)-PK11195 shows increased binding in regions traditionally not associated with activated brain macrophages in regions such as the thalamus in Alzheimer's disease (Cagnin et al., 2001), Parkinson's disease (Ouchi et al., 2005) and Huntington's disease (Pavese et al., 2006), and the occipital cortex in amyotrophic lateral sclerosis (Turner et al., 2004). Since it is not possible to confirm the histopathological presence of activated brain macrophages in these regions in human PET studies, it is possible that these findings reflect activated brain macrophages in regions connected by synapses to areas of pathology. Alternatively, they may represent regional variations in the constitutive PBR or some degree of non-uniform non-specific binding in the CNS. These concerns along with the possibility of low sensitivity in milder forms of neuroinflammation highlight the importance of developing newer ligands that show more specificity and sensitivity to activated brain macrophages for PET imaging in diseases such as HIVE. [^{3}H]DAA1106 binds with higher B_{max}/K_D ratios in comparison to PK11195 to activated and infected macrophages in lentiviral encephalitis in areas of synaptic damage suggesting that DAA1106 possesses better binding characteristics over PK11195 for labeling activated and infected macrophages in lentiviral encephalitis. It is possible that filtration binding experiments in brain tissues may not be entirely reflective of *in vivo* properties of the ligand. Various parameters such as the ability of a given ligand to cross the blood brain barrier, *in vivo* binding kinetics to PBR, issues of *in vivo* non specific binding and the rate of metabolism of the ligand influence the utility of the ligand in question as a PET tracer. We are currently conducting experiments in macaques infected with SIV using [^{11}C] DAA1106 to address these points. Nevertheless, the assertion that a PET radioligand with potential clinical utility is binding to the intended cellular component; activated and infected brain macrophages, and that changes in measured B_{max} values determined using a standardized assay are observed in a manner that is consistent with the known disease pathology is an important validation that is often overlooked or bypassed in the progression to human investigational studies. Overall, these results suggest that DAA1106 has binding characteristics that might offer improved sensitivity to image activated and infected macrophages in lentiviral encephalitis *in vivo* using PET. Further studies in HIV infected human subjects with and without neurological impairments are required to fully characterize the potential enhancements of DAA1106.

Acknowledgements

We thank James Kasenchak, Jason Nugyen and Susan Slagel for technical help, Brian Lopresti for helpful comments, Dr. Stephanie J. Bissel for banking macaque brain tissues, Dr. Ronald L. Hamilton, Jonette Werley and the University of Pittsburgh brain bank for human post mortem tissues. This work was supported by the National Institutes of Health: RO1 MH64921 (CAW), K24 MH01717 (CAW).

References

Abe K, Saito H. The p44/42 mitogen-activated protein kinase cascade is involved in the induction and maintenance of astrocyte stellation mediated by protein kinase C. Neurosci Res 2000;36:251–257. [PubMed: 10683529]

Banati RB. Visualising microglial activation in vivo. Glia 2002;40:206–217. [PubMed: 12379908]

Banati RB, Newcombe J, Gunn RN, Cagnin A, Turkheimer F, Heppner F, Price G, Wegner F, Giovannoni G, Miller DH, Perkin GD, Smith T, Hewson AK, Bydder G, Kreutzberg GW, Jones T, Cuzner ML, Myers R. The peripheral benzodiazepine binding site in the brain in multiple sclerosis: quantitative in vivo imaging of microglia as a measure of disease activity. Brain 2000;123(Pt 11):2321–2337. [PubMed: 11050032]

Barami K, Grever WE, Diaz FG, Lyman WD. An efficient method for the culturing and generation of neurons and astrocytes from second trimester human central nervous system tissue. Neurol Res 2001;23:321–326. [PubMed: 11428508]

Bergamini A, Faggioli E, Bolacchi F, Gessani S, Cappannoli L, Uccella I, Demin F, Capozzi M, Cicconi R, Placido R, Vendetti S, Colizzi GM, Rocchi G. Enhanced production of tumor necrosis factor-alpha and interleukin-6 due to prolonged response to lipopolysaccharide in human macrophages infected in vitro with human immunodeficiency virus type 1. J Infect Dis 1999;179:832–842. [PubMed: 10068578]

Brew BJ, Rosenblum M, Cronin K, Price RW. AIDS dementia complex and HIV-1 brain infection: clinical-virological correlations. Ann Neurol 1995;38:563–570. [PubMed: 7574452]

Budka H. Neuropathology of human immunodeficiency virus infection. Brain Pathol 1991;1:163–175. [PubMed: 1669705]

Cagnin A, Gerhard A, Banati RB. In vivo imaging of neuroinflammation. Eur Neuropsychopharmacol 2002;12:581–586. [PubMed: 12468021]

Cagnin A, Brooks DJ, Kennedy AM, Gunn RN, Myers R, Turkheimer FE, Jones T, Banati RB. In-vivo measurement of activated microglia in dementia. Lancet 2001;358:461–467. [PubMed: 11513911]

Casellas P, Galiegue S, Basile AS. Peripheral benzodiazepine receptors and mitochondrial function. Neurochem Int 2002;40:475–486. [PubMed: 11850104]

Chaki S, Funakoshi T, Yoshikawa R, Okuyama S, Okubo T, Nakazato A, Nagamine M, Tomisawa K. Binding characteristics of [3H]DAA1106, a novel and selective ligand for peripheral benzodiazepine receptors. Eur J Pharmacol 1999;371:197–204. [PubMed: 10357257]

Chen MK, Baidoo K, Verina T, Guilarte TR. Peripheral benzodiazepine receptor imaging in CNS demyelination: functional implications of anatomical and cellular localization. Brain 2004;127:1379–1392. [PubMed: 15069023]

Cinque P, Scarpellini P, Vago L, Linde A, Lazzarin A. Diagnosis of central nervous system complications in HIV-infected patients: cerebrospinal fluid analysis by the polymerase chain reaction. Aids 1997;11:1–17. [PubMed: 9110070]

Dore GJ, Correll PK, Li Y, Kaldor JM, Cooper DA, Brew BJ. Changes to AIDS dementia complex in the era of highly active antiretroviral therapy. Aids 1999;13:1249–1253. [PubMed: 10416530]

Ellis R, Langford D, Masliah E. HIV and antiretroviral therapy in the brain: neuronal injury and repair. Nat Rev Neurosci 2007;8:33–44. [PubMed: 17180161]

Geraci AP, Simpson DM. Neurological manifestations of HIV-1 infection in the HAART era. Compr Ther 2001;27:232–241. [PubMed: 11569325]

Gray F, Keohane C. The neuropathology of HIV infection in the era of Highly Active AntiRetroviral Therapy (HAART). Brain Pathol 2003a;13:79–83. [PubMed: 12580547]

Gray F, Chretien F, Vallat-Decouvelaere AV, Scaravilli F. The changing pattern of HIV neuropathology in the HAART era. J Neuropathol Exp Neurol 2003b;62:429–440. [PubMed: 12769183]

Groom GN, Junck L, Foster NL, Frey KA, Kuhl DE. PET of peripheral benzodiazepine binding sites in the microgliosis of Alzheimer's disease. J Nucl Med 1995;36:2207–2210. [PubMed: 8523106]

Hammoud DA, Endres CJ, Chander AR, Guilarte TR, Wong DF, Sacktor NC, McArthur JC, Pomper MG. Imaging glial cell activation with [11C]-R-PK11195 in patients with AIDS. J Neurovirol 2005;11:346–355. [PubMed: 16162478]

Itzhak Y, Norenberg MD. Regulation of peripheral-type benzodiazepine receptors in cultured astrocytes by monoamine and amino acid neurotransmitters. Brain Res 1994;660:346–348. [PubMed: 7820705]

Kuhlmann AC, Guilarte TR. Cellular and subcellular localization of peripheral benzodiazepine receptors after trimethyltin neurotoxicity. J Neurochem 2000;74:1694–1704. [PubMed: 10737628]

Lackner AA, Smith MO, Munn RJ, Martfeld DJ, Gardner MB, Marx PA, Dandekar S. Localization of simian immunodeficiency virus in the central nervous system of rhesus monkeys. Am J Pathol 1991;139:609–621. [PubMed: 1716047]

Langford TD, Letendre SL, Larrea GJ, Masliah E. Changing patterns in the neuropathogenesis of HIV during the HAART era. Brain Pathol 2003;13:195–210. [PubMed: 12744473]

Lee SC, Liu W, Brosnan CF, Dickson DW. Characterization of primary human fetal dissociated central nervous system cultures with an emphasis on microglia. Lab Invest 1992;67:465–476. [PubMed: 1359193]

Maeda J, Suhara T, Zhang MR, Okauchi T, Yasuno F, Ikoma Y, Inaji M, Nagai Y, Takano A, Obayashi S, Suzuki K. Novel peripheral benzodiazepine receptor ligand [11C]DAA1106 for PET: An imaging tool for glial cells in the brain. Synapse 2004;52:283–291. [PubMed: 15103694]

Mankowski JL, Queen SE, Tarwater PJ, Adams RJ, Guilarte TR. Elevated peripheral benzodiazepine receptor expression in simian immunodeficiency virus encephalitis. J Neurovirol 2003;9:94–100. [PubMed: 12587072]

Masliah E, Heaton RK, Marcotte TD, Ellis RJ, Wiley CA, Mallory M, Achim CL, McCutchan JA, Nelson JA, Atkinson JH, Grant I, HNRC Group; The HIV Neurobehavioral Research Center. Dendritic injury is a pathological substrate for human immunodeficiency virus-related cognitive disorders. Ann Neurol 1997;42:963–972. [PubMed: 9403489]

Mintun MA, Raichle ME, Kilbourn MR, Wooten GF, Welch MJ. A quantitative model for the in vivo assessment of drug binding sites with positron emission tomography. Ann Neurol 1984;15:217–227. [PubMed: 6609679]

Nath A, Sacktor N. Influence of highly active antiretroviral therapy on persistence of HIV in the central nervous system. Curr Opin Neurol 2006;19:358–361. [PubMed: 16914973]

Ouchi Y, Yoshikawa E, Sekine Y, Futatsubashi M, Kanno T, Ogusu T, Torizuka T. Microglial activation and dopamine terminal loss in early Parkinson's disease. Ann Neurol 2005;57:168–175. [PubMed: 15668962]

Padmanabhan J, Clayton D, Shelanski ML. Dibutyryl cyclic AMP-induced process formation in astrocytes is associated with a decrease in tyrosine phosphorylation of focal adhesion kinase and paxillin. J Neurobiol 1999;39:407–422. [PubMed: 10363913]

Pappata S, Levasseur M, Gunn RN, Myers R, Crouzel C, Syrota A, Jones T, Kreutzberg GW, Banati RB. Thalamic microglial activation in ischemic stroke detected in vivo by PET and [11C]PK1195. Neurology 2000;55:1052–1054. [PubMed: 11061271]

Pavese N, Gerhard A, Tai YF, Ho AK, Turkheimer F, Barker RA, Brooks DJ, Piccini P. Microglial activation correlates with severity in Huntington disease: a clinical and PET study. Neurology 2006;66:1638–1643. [PubMed: 16769933]

Petit-Taboue MC, Baron JC, Barre L, Travere JM, Speckel D, Camsonne R, MacKenzie ET. Brain kinetics and specific binding of [11C]PK 11195 to omega 3 sites in baboons: positron emission tomography study. Eur J Pharmacol 1991;200:347–351. [PubMed: 1782994]

Schuitemaker A, Van Berckel BN, Kropholler M, Boellaard R, Jonker C, Scheltens P, Lammertsma AA. Microglia activation in mild cognitive impairment. Neurobiol. of Aging 2004;25(Suppl2):S286.

Schuitemaker A, Van Berckel BN, Boellaard R, Kropholler M, Boellaard R, Jonker C, Lubberlink M, Scheltens P, Lammertsma AA. Assessment of microglial activation in mild cognitive impairment using [11C](R)-PK11195 and PET. Neuroimage 2006;31:T159.

Taylor SW, Fahy E, Zhang B, Glenn GM, Warnock DE, Wiley S, Murphy AN, Gaucher SP, Capaldi RA, Gibson BW, Ghosh SS. Characterization of the human heart mitochondrial proteome. Nat Biotechnol 2003;21:281–286. [PubMed: 12592411]

Turner MR, Cagnin A, Turkheimer FE, Miller CC, Shaw CE, Brooks DJ, Leigh PN, Banati RB. Evidence of widespread cerebral microglial activation in amyotrophic lateral sclerosis: an [11C](R)-PK11195 positron emission tomography study. Neurobiol Dis 2004;15:601–609. [PubMed: 15056468]

Valcour VG, Shikuma CM, Watters MR, Sacktor NC. Cognitive impairment in older HIV-1-seropositive individuals: prevalence and potential mechanisms. Aids 2004;18(Suppl 1):S79–86. [PubMed: 15075502]

Venneti S, Lopresti BJ, Wiley CA. The peripheral benzodiazepine receptor (Translocator protein 18kDa) in microglia: From pathology to imaging. Prog Neurobiol. 2006

Venneti S, Lopresti BJ, Wang G, Bissel SJ, Mathis CA, Meltzer CC, Boada F, Capuano S 3rd, Kress GJ, Davis DK, Ruszkiewicz J, Reynolds IJ, Murphey-Corb M, Trichel AM, Wisniewski SR, Wiley CA. PET imaging of brain macrophages using the peripheral benzodiazepine receptor in a macaque model of neuroAIDS. J Clin Invest 2004;113:981–989. [PubMed: 15057304]

Wiley CA, Lopresti BJ, Becker JT, Boada F, Lopez OL, Mellors J, Meltzer CC, Wisniewski SR, Mathis CA. Positron emission tomography imaging of peripheral benzodiazepine receptor binding in human immunodeficiency virus-infected subjects with and without cognitive impairment. J Neurovirol 2006;12:262–271. [PubMed: 16966217]

Zhang MR, Kida T, Noguchi J, Furutsuka K, Maeda J, Suhara T, Suzuki K. [(11)C]DAA1106: radiosynthesis and in vivo binding to peripheral benzodiazepine receptors in mouse brain. Nucl Med Biol 2003;30:513–519. [PubMed: 12831989]

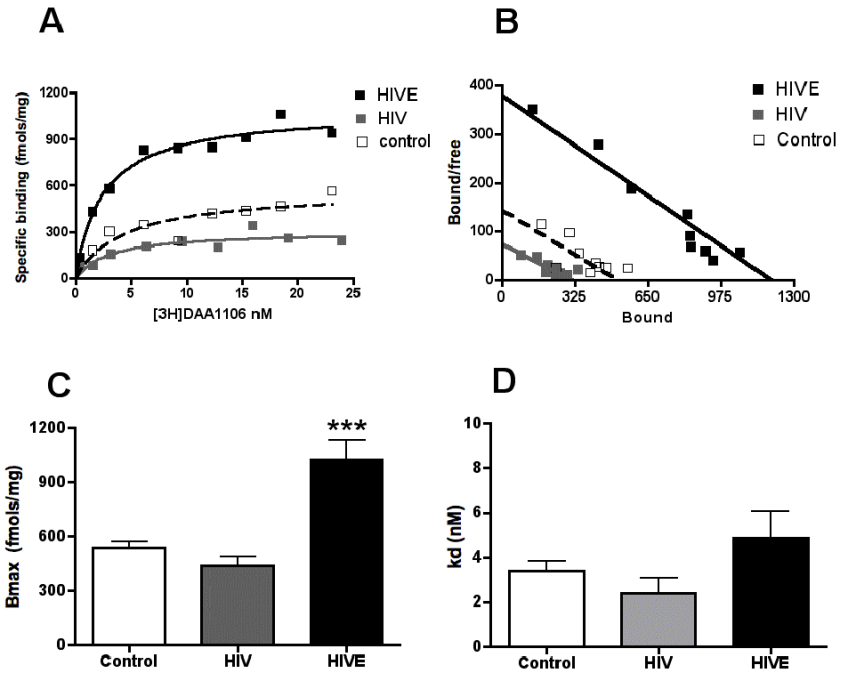

Figure 1. [^{3}H]DAA1106 binding is higher in HIVE compared to controls

Saturation filtration binding experiments were performed in basal ganglia tissues from HIVE (n=5), HIV non-encephalitis (HIV, n=6) and age-matched non-infected controls (n=3).

A & B, Representative saturation binding curves (**A**) and schatchard plots (**B,** X-intercept represent B_{max}, and slope represents K_D) with [^{3}H]DAA1106 from HIVE (black squares), HIV no-encephalitis (grey squares) and an age-matched control (clear squares).

C, The B_{max} (fmols/mg) reflective of the total number of binding sites, with [^{3}H]DAA1106 was significantly higher in HIVE (black bars) compared with HIV non-encephalitis (grey bars) and non-infected controls (clear bars), p=0.0003.

D, The K_D (nM), reflective of the ligand binding affinity was not significantly different in all three conditions, p=0.0712. Data was analyzed using ANOVA.

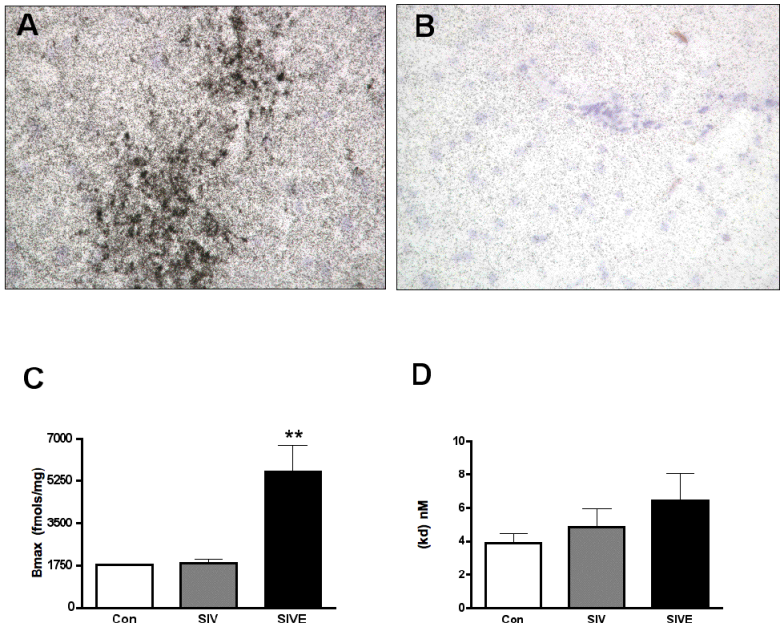

Figure 2. [^{3}H]DAA1106 binding is higher in SIVE compared to controls

A & B, [^{3}H]DAA1106 autoradiographic binding assessed in the frontal cortex of macaques with SIVE corresponded to the distribution of microglial nodules (**A**) and was specific as it was displaced by 1 nM DAA1106 (**B**).

C & D, B_{max} (fmols/mg) with [^{3}H]DAA1106 was significantly higher in SIVE (n=3, black bars) compared with SIV non-encephalitis (n=4, grey bars) and non-infected controls (n=3, clear bars), p=0.0038 (**C**). The K_D (nM) was not significantly different in all three conditions, p=0.2492, (**D**). Data was analyzed using ANOVA.

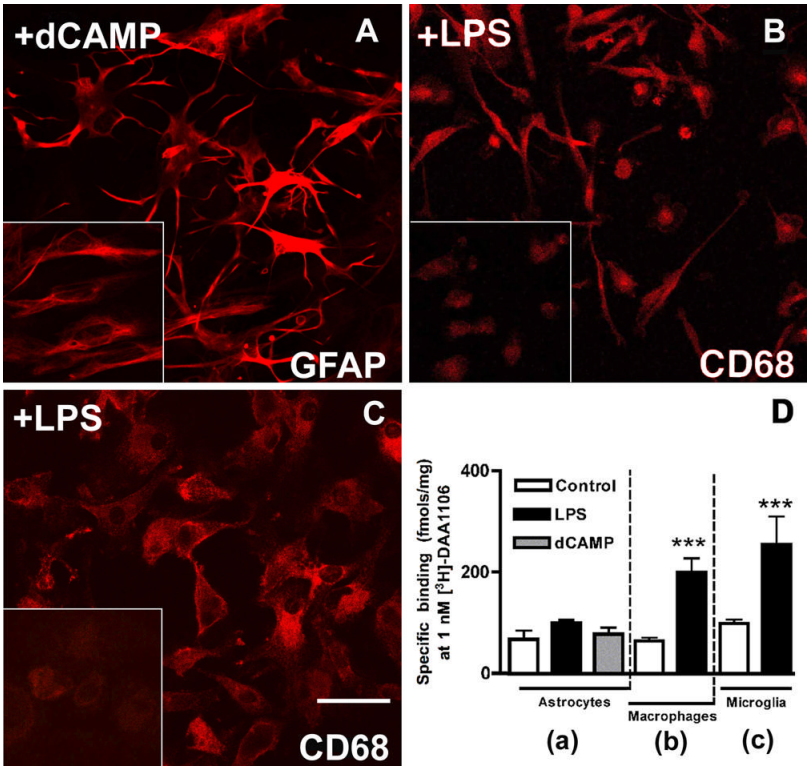

Figure 3. Primary human microglia and macrophages, but not astrocytes show increased [^{3}H] DAA1106 binding on activation

A, Primary human embryonic astrocytes activated with dB-cAMP show changes in morphology with the appearance of spindle shaped processes and increased GFAP staining compared to non-activated cultures (inset).

B, Primary human macrophages activated with LPS show changes in morphology from a rounded shape (inset) to spindle shaped with increased CD68 staining in non-stimulated cultures.

C, Primary human embryonic microglia were activated with LPS for 48 hrs show increased CD68 staining compared to non-activated cultures (inset).

D, [^{3}H]DAA1106 specific binding (fmols/mg mitochondrial protein) was significantly higher in mitochondrial preparations obtained from both macrophages (**b**) and microglia (**c**) activated with LPS (black bars) compared to unactivated controls (white bars) and astrocytes (**a**) with or without activation. Data was analyzed using ANOVA, n=3 in each group, ***p<0.0001.

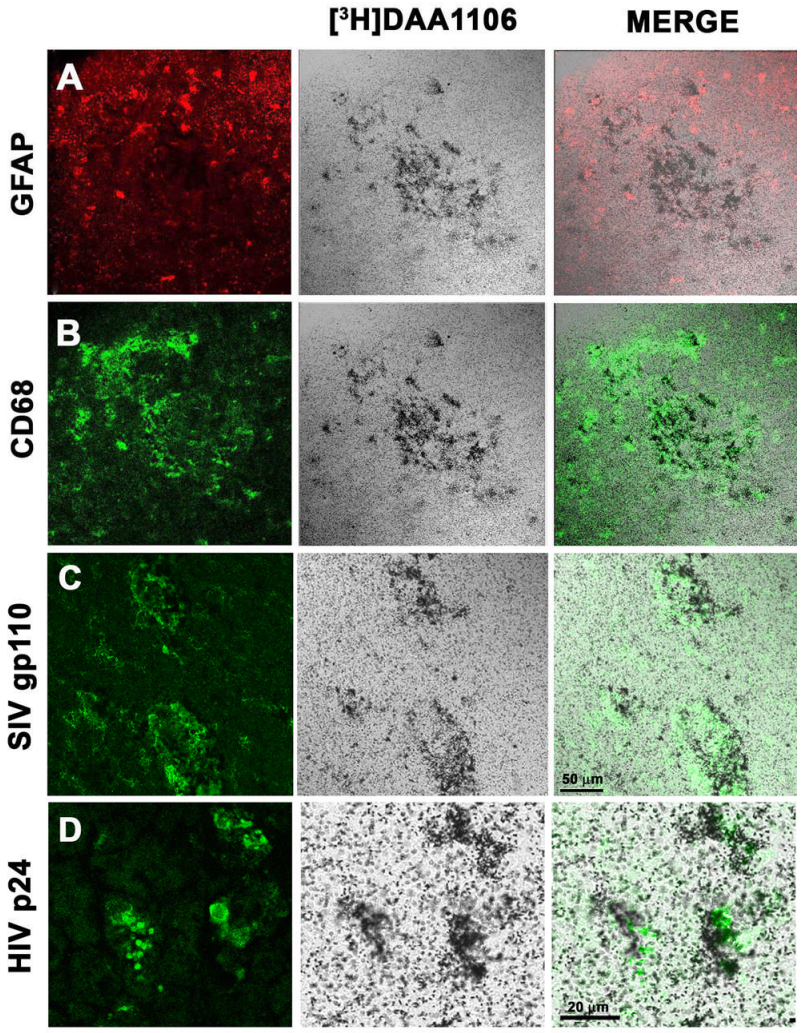

Figure 4. [^{3}H]DAA1106 binding corresponds to activated and infected macrophages in SIVE

A-C, Combined [^{3}H]DAA1106 autoradiography (center panel, black grains) and immunostaining for astrocytes (**A**, GFAP, red), activated macrophages (**B**, CD68, green) and SIV infected cells (**C**, SIV gp110, green) was performed in cortical brain tissue obtained from macaques with SIVE. [^{3}H]DAA1106 specific binding overlapped with CD68 labeled activated macrophages (**C**, merge) and SIV infected macrophages (**D**, merge), but not with GFAP immunostained astrocytes (**A**, Merge). Scale bar indicates 50 μm.

D, Combined [^{3}H]DAA1106 autoradiography (center panel, black grains) and immunostaining for HIV p24 (green) in HIVE basal ganglia showed [^{3}H]DAA1106 specific binding overlapping with HIV infected macrophages (merge). Scale bar indicates 20 μm.

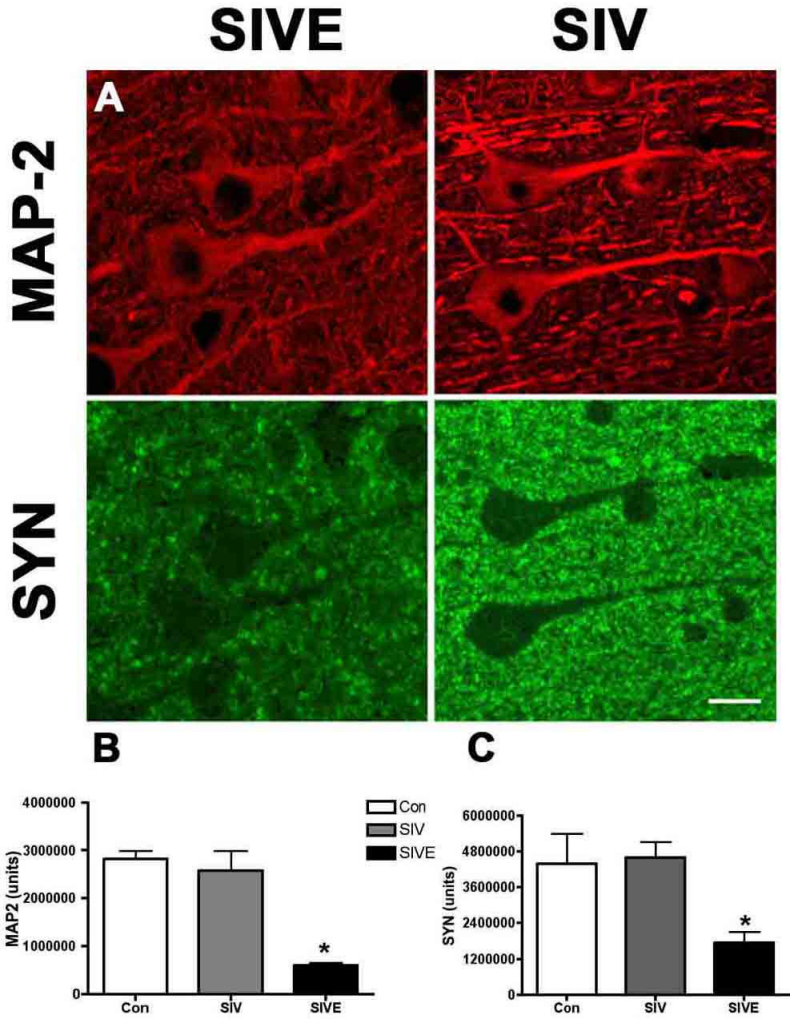

Figure 5. [^{3}H]DAA1106 specific binding correlates with decreases in the presynaptic protein SYN and the postsynaptic protein MAP-2

A, The postsynaptic protein MAP-2 (Red) a marker for dendrites and neuronal cell bodies and presynaptic protein SYN (green) were lower in SIVE compared to SIV non-encephalitis (SIV). **B-C,** Quantification of these markers showed significant decreases in MAP-2 (**B**) and SYN (**C**) in SIVE (n=3, black bars) compared to SIV non-encephalitis (SIV, n=4, grey bars) and non-infected controls (Con, n=3, clear bars). Data was analyzed using student *t* test ANOVA, *p<0.05.

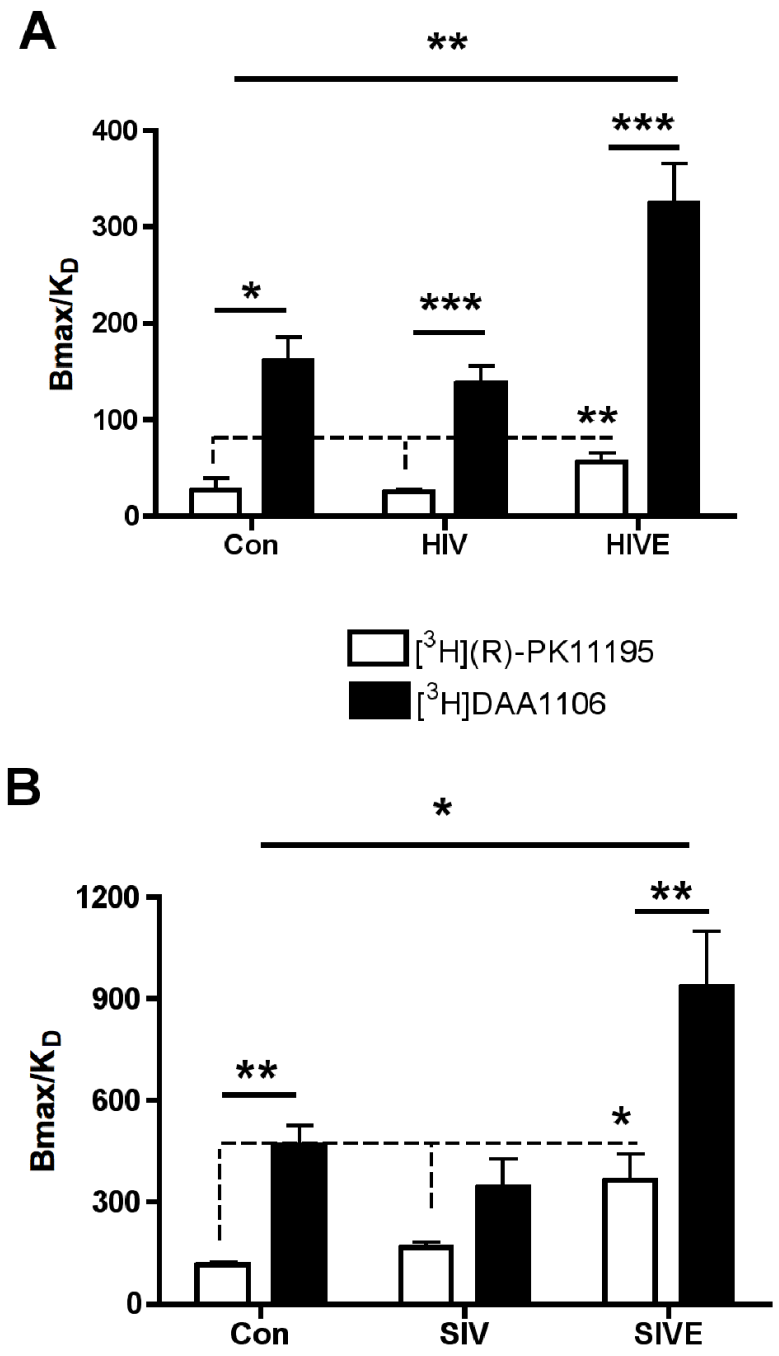

Figure 6. [^{3}H]DAA1106 B_{max}/K_D ratios are significantly higher than that of [^{3}H](R)-PK11195 in lentiviral encephalitis

A & B, The ratio of B_{max}/K_D (representing the binding potential) was significantly higher with either [^{3}H]DAA1106 (black bars and line) or [^{3}H](R)-PK11195 (clear bars and dotted line) in HIVE (n=5) compared to HIV non-encephalitis (HIV, n=6) and age-matched non-infected controls (Con, n=3) (**A**), and in SIVE (n=3) compared to SIV non-encephalitis (SIV, n=4) and non-infected controls (Con, n=3) (**B**). Data was analyzed using one-way ANOVA between the three conditions with either ligand. The B_{max}/ K_D ratio with [^{3}H]DAA1106 was significantly higher compared to [^{3}H](R)-PK11195 within each condition with the greatest obsereved

differences in encephalitic tissues. Data was analyzed using student's *t* test within the same condition, ***p<0.01**p<0.01, *p<0.05.

Table 1

Demographics of archival human and macaque post mortem tissue

Neuropathological diagnosis	ID #	Age (years)	Sex	PMI (h)	ART	Cause of Death
HIV encephalitis	1021	31	M	21	None	UN
	3067	28	M	18	None	Kaposi sarcoma lung
	3099	36	M	23	None	CMV adrenalitis
	5087	47	M	24	None	Aplastic anemia
	9030	UN	M	18	UN	UN
HIV non-encephalitis	4044	43	M	20	None	Hepatic failure due to cirrhosis
	4084	39	M	10	None	Cardiac failure
	4097	33	M	12	AZT- 1year	CMV adrenalitis
	4144	32	M	20	None	Acute peritonitis due to Small bowel perforation
	9081	55	M	25	None	Diabetic ketoacidosis
Control	3182	69	M	<24	NA	Acute non lymphocytic leukemia
	3186	60	M	<24	NA	Surgical complications of liver transplant
	3188	54	F	<24	NA	Myocardial infarction
Neuropathological diagnosis	**ID #**	**Age (mo.)**	**Sex**	**Length of infection (days)**	**Disease at time of sacrifice**	**Clinical symptoms**
SIV encephalitis	13901	34	M	56	AIDS	Anorexia and diarrhea
	14001	46	M	56	AIDS	Anorexia and diarrhea
	16103	59	M	119	AIDS	Ataxia and pneumocystitis pneumonia
SIV non-encephalitis	10797	168	F	722	AIDS	Anorexia
	14101	22	M	101	AIDS	Diarrhea
	15201	39	M	30	Asymptomatic	Diarrhea
	17000	84	F	1062	AIDS	Anorexia and diarrhea
Control	40500	UN	M	NA	NA	NA
	42100	66	F	NA	NA	NA
	42200	UN	UN	NA	NA	NA

PMI (h) - Post mortem interval in hours, M - male, F - Female, ART - Antiretroviral therapy, AZT - azidothymidine, CMV- cytomegalovirus, mo. - months, UN - Unknown, NA - Not applicable.

Table 2

[^{3}H]DAA1106 binding correlates with activated and infected brain macrophages and areas of synaptic damage

Parameter	Marker	*r* value	*p* value
Activated macrophages	CD68	0.8308	0.0106
Infected macrophages	SIV gp110	0.9646	0.0084
Reactive astrocytosis	GFAP	0.6755	0.0958
Presynaptic protein	SYN	-0.7806	0.0383
Postsynaptic protein	MAP-2	-0.7868	0.0205

[^{3}H]DAA1106 B_{max} values in SIVE and SIV brain tissues were correlated with changes in the abundance of activated (CD68) and infected macrophages (SIV gp110) or (GFAP) or with the synaptic markers (SYN and MAP-2) in the frontal cortical of the same cases. Increases in [^{3}H]DAA1106 binding correlated best with activated and infected macrophages. Increase in [^{3}H]DAA1106 binding correlated significantly with decreases in both presynaptic and postsynaptic markers.

Table 3

Comparison of [^{3}H](R)-PK11195 and [^{3}H]DAA1106 B_{max} and K_D values in human and macaque postmortem tissues

	B_{max} (fmols/mg)			K_D (nM)		
Condition	**[^{3}H]DAA1106**	**[^{3}H](R)-PK11195**	***p* value**	**[^{3}H]DAA1106**	**[^{3}H](R)-PK11195**	***p* value**
Control	1775 ± 46	2030 ± 74	0.0526	3.5 ± 0.5	17 ± 0.2	**0.0004**
SIV	1856 ± 165	2299 ± 149	0.1290	4.8 ± 0.9	14 ± 1.8	**0.0080**
SIVE	5631 ± 946**	4815 ± 626**	0.5238	6.4 ± 1.3	18 ± 4.3	**0.0320**
Control	536 ± 34	649 ± 275	0.6280	3.4 ± 0.6	24 ± 1.0	**0.0002**
HIV	448 ± 69	848 ± 139	0.1010	3.3 ± 0.5	32 ± 2.6	**0.0004**
HIVE	1158 ± 104***	1660 ± 105***	0.2074	4.8 ± 1.3	30 ± 4.1	**0.0037**

B_{max} (reflective of the total number of binding sites) and K_D (inversely proportional to the binding affinity) were compared in macaque and human brain tissues using [^{3}H]DAA1106 and [^{3}H](R)-PK11195. With each ligand, B_{max} values were significantly higher in encephalitis compared to controls (***p<0.01, **p<0.01 data was analyzed using ANOVA). B_{max} values were not significantly different between [^{3}H]DAA1106 and [^{3}H](R)-PK11195 in any of the conditions. K_D values were significantly lower with [^{3}H]DAA1106 compared to [^{3}H](R)-PK11195 in all the conditions (data was analyzed using students *t* test).